JOURNAL OF CATALYSIS 82, 322–331 (1983)

Interpretation of the Electromotive Forces of Solid Electrolyte Concentration Cells during Carbon Monoxide Oxidation on Platinum

HIROSHI OKAMOTO, GO KAWAMURA, AND TETSUICHI KUDO

Central Research Laboratory, Hitachi Ltd., 1-280, Higashi-Koigakubo, Kokubunji, Tokyo 185, Japan

Received March 9, 1982; revised July 14, 1982

The electromotive force (emf) of solid electrolyte concentration cells used in CO + O_2 nonequilibrium conditions has been studied by comparing the behavior of the reaction rate and emf for deposited Pt with that of the reaction rate and surface concentration of CO (as determined by infrared spectroscopy) for dispersed Pt. It was confirmed that the emf is generated by a mixed electrode potential involving electrochemical reactions of O^{2-} with the CO and oxygen adsorbed on Pt during CO oxidation on Pt. Taking this mechanism as a basis for investigation, surface CO was detected even under conditions where CO was very scarce compared to oxygen. This indicates that CO oxidation on Pt proceeds via a Langmuir–Hinshelwood mechanism involving surface reaction between adsorbed species over the whole range of gas composition. Oscillations in emf, rate, and surface concentration of CO shown over a certain range of gas composition were presumed to be caused by the surface state where CO adsorbed on Pt became mobile.

INTRODUCTION

A galvanic cell of the type:

$$O_2(P_{O_2}) + CO(P_{CO}),\ \text{Pt/stabilized } ZrO_2\text{/Pt},\ O_2(P'_{O_2}), \quad (1)$$

is expected to give an emf, E, according to the Nernst equation, of

$$E = \left|\frac{RT}{4F} \ln (P'_{O_2}/P''_{O_2})\right|. \quad (2)$$

Here, R is the molar gas constant, T the absolute temperature, F the Faraday constant, and P''_{O_2} is the equilibrium O_2 partial pressure for a mixed gas in the reaction

$$2CO + O_2 = 2CO_2. \quad (3)$$

A galvanic cell type (1) shows a curve with an emf gap for the stoichiometric ratio of Reaction (3) at high temperatures, when the equilibrium of this reaction is established. At low temperatures around 600°K, however, the emf deviates significantly from that calculated using Eq. (2). Particularly in the region $P_{CO}/P_{O_2} < 2$, an anomalously high emf is observed (*1–4*). This high emf is caused by imperfect catalytic activity for a platinum electrode (*1–4*). It is thought to reflect either the adsorption states of CO and oxygen on Pt (*2–4*) or oxygen activity on Pt (*5–8*) during the reaction. Accordingly, in either case, emf measurements are useful for investigating surface adsorption states during the reaction. The importance of such investigations has been emphasized for the study of heterogeneous catalysis by Tamaru (*9*).

Rate equations for the oxidation of CO on Pt are similar both at very low pressures between 10^{-6} and 10^{-3} Pa, and at high pressures of the order of 1 kPa. They possess first-order P_{CO} and inhibition regions (10). However, the transition point between these regions shifts from about 1 to about 0.1 in the partial pressure ratio, P_{CO}/P_{O_2}, as the pressures are increased by several orders of magnitude. Moreover, oscillations in the oxidation occur over a certain range of gas composition at high pressures (*2–4, 12–14*). In this way some features of CO oxidation are different due only to the partial pressures. Therefore studies of these phenomena are very significant when results in the field of surface science are

0021-9517/83 $3.00

applied to the field of "real catalysts." Electromotive-forces measurements are in principle possible over a wide range in pressure from ultra-high vacuum (UHV) to above atmopsheric pressures. Accordingly, emf can be useful also in studying oxidation over a wide pressure range.

To connect emf with surface adsorption quantities, the mechanism for emf generation is discussed in this paper. Mechanisms for CO oxidation and its oscillation are also briefly discussed. The mechanism for the emf production was studied by comparing the behavior of the reaction rate and emf for deposited Pt of a solid electrolyte cell type (1) with the behavior of the reaction rate and surface concentration of CO for dispersed Pt. This procedure has been employed by Heyne and Tompkins (*15*) and by Okamoto *et al.* (*4*). In the latter paper, the same subject was looked at with the aid of a closed circulating system for studying the oxidation; however, the behavior of first-order P_{CO} and oscillation regions remained rather obscure. In the present paper flowing gas was used for studying the oxidation both on the deposited and dispersed Pt.

EXPERIMENTAL

a. Sample preparation. Two kinds of sample were employed. One was a solid electrolyte cell. The other was dispersed Pt on a support for infrared spectral studies.

The solid electrolyte cell was made in the following way (*3, 4*). Y_2O_3-stabilized ZrO_2 was used as a solid electrolyte. Eight mole percents of Y_2O_3 (99.9%, Kojundo Kagaku Co.) and 92 mol% of ZrO_2 (99.2%, Daiichi Kido Kagaku Co.) were mixed with 1 wt% of SiO_2 (Kojundo Kagaku Co.) and then the mixture was calcined at 1770°K for 1 h. The calcined specimen was pulverized and 3 g of the powder were pressed into a pellet, 25 mm in diameter, and sintered at 1870°K for 3 h. The sintered pellet was about 1-mm thick and about 20 mm in diameter. The apparent density was 94–95% of the theoretical calculation based on X-ray diffraction.

Before it was provided with Pt electrodes, the sample was polished on both sides by an SiC abrasive (particle size: 7.9 μm). Platinum electrodes were deposited by electron-beam evaporation on both sides of the pellet at 520°K. Typical electrodes were 0.1-μm thick and 12 mm in diameter.

The supported sample of dispersed Pt was prepared in the following manner. The Pt content was 3 wt% and the support was Y_2O_3 (6.9 mol%)-stabilized ZrO_2 (Zircar Products, Inc.; specific surface area = 40–60 m^2g^{-1}, particle size = 20–30 nm), which was different from that of the solid electrolyte cell for experimental convenience. The yttria-stabilized ZrO_2 powder was impregnated with H_2PtCl_6 (Mitsuwa Junyaku Co.) aqueous solution and pressed into a pellet with a diameter of 2 cm. After the pellet was reduced with a gas flow including 6% H_2 (N_2 base) at 770°K for 0.5 h in a cell set up for infrared spectroscopy, the sample was treated with O_2 (6%) at the same temperature for 0.5 h, in order to make its surface state similar to that of the solid electrolyte cell.

b. Experimental set-up. Figure 1 shows the apparatus employed to measure emf and surface temperature. The solid electrolyte cell was held horizontal between vertical glass tubes by springs so as to keep the system gastight.

Air was fed onto the upper surface of the specimen (air electrode), and a mixed gas of CO, O_2, and N_2 was passed over the other

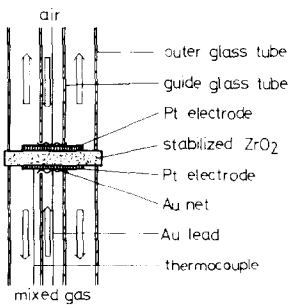

FIG. 1. Solid electrolyte concentration cell setup employed for emf and surface temperature measurements.

surface (mixed-gas electrode). All gases were supplied from commercially available gas cylinders without any special purification. Their purity levels were: N_2, 99.9995% (Nihon Sanso Co.); H_2, 99.99% (Showa Denko Co.); O_2, 99.99% (Nihon Sanso Co.); and CO, 99.9% (Seitetsu Kagaku Co.) with 1% CO/N_2 and 10% CO/N_2 (Nihon Sanso Co.). These gases were appropriately mixed with a thermal mass flow control system (Nippon tylan, to within an accuracy of ±0.25%). The linear velocity of each gas was 1.7 m s^{-1} (296°K). Air or a gas mixture flowed through a guide glass tube onto the specimen surface and then out into an outer glass tube through four narrow openings in the guide glass tube near the specimen surface.

The furnace temperature was proportional, integral, and differential (PID) controlled to within ±0.02°K. The electrodes were contacted with catalytically inactive gold net leads. The emf was recorded via an impedance converter (Nikko Keisoku Co., Type IC-2, nominal impedance 10^{10} Ω) by a recorder (Hitachi Ltd., Type 056). The Pt surface temperature of the mixed-gas electrode was monitored by a catalytically inactive thermocouple, chromel–alumel, and recorded simultaneously with the emf. Small temperature changes on the surface were measured via a laboratory-made small voltage difference meter (to within an accuracy of ±0.05°K).

A cylindrical cell made of quartz glass was used for infrared spectroscopic measurement of surface-adsorbed CO. The cell was a conventional one with a heating wire outside the cylinder, and NaCl windows at both ends of the cell. The cell temperature was PID-controlled to within ±0.02°K. The sample temperature, and small changes in it, were monitored and recorded and the gas was mixed in the same way as for the emf measurement. Infrared spectra were recorded with a Hitachi grating infrared spectrophotometer, Model EPI G3, with a resolution of 2 cm^{-1}.

The content of CO_2 in the effluent gas was determined by the absorbance at 2360 cm^{-1} using a gas cell. Residence time for flowing gas in the gas cell was about 2 s. The reactor for the CO_2 content measurement was a differential one including a sample pellet whose temperature was monitored and recorded in the same way as for the emf measurement.

RESULTS

a. CO Oxidation on Deposited Pt of a Solid Electrolyte Cell

Figure 2 shows the emf and the temperature difference on the Pt surface, ΔT, between the temperature in the absence of CO, T_O, and that in the presence of CO, T, for a solid electrolyte cell type (1) with deposited Pt. Conditions are T_O = 603°K and P_{O_2} = 5 kPa. ΔT, which is generated by the heat of reaction, can be considered to be proportional to the reaction rate, so long as ΔT is sufficiently small and a thermal steady state is established.

The same temperature change as that in Fig. 2 was observed on deposited Pt on SiO_2. Thus, ΔT observed here can be regarded as indicating the chemical oxidation rate, not the rate for the electrochemical reactions near a triple contact Pt-stabilized ZrO_2-gas. This is because the progress of

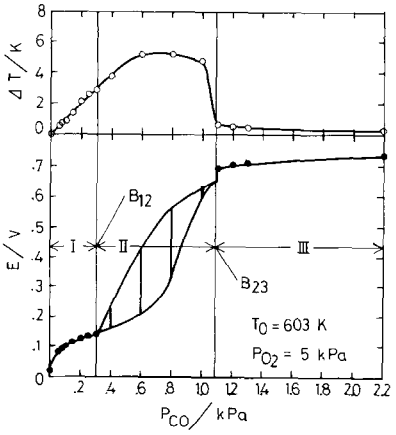

FIG. 2. Emf (E) and surface temperature increase (ΔT) for solid electrolyte concentration cell with fixed P_{O_2}. T_O: surface temperature in absence of CO; T: surface temperature in presence of CO; $\Delta T = T - T_O$.

electrochemical reactions on Pt/SiO_2 is considered to be much less than that for Pt/stabilizing ZrO_2.

When P_{CO} starts out from zero and is then increased to a certain value (0.3 kPa in this case), E increases. However, its slope decreases, and ΔT increases linearly with P_{CO}. This portion of P_{CO} at a given P_{O_2} will hereafter be called region I. In a certain range of P_{CO} (from 0.3 to 1.1 kPa in this case), E oscillates. This gives the E range shown in Fig. 2, and this region is designated region II. It has a lower boundary at B_{12} and a higher boundary at B_{23}. These boundaries will be discussed in connection with transitions of surface adsorption states. There are several types of oscillation patterns, some of which have been illustrated elsewhere (*2, 4*). ΔT also oscillates to a small extent, ca. ±0.1°K, and shows a maximum in this region. At B_{23}, E stops oscillating abruptly and ΔT decreases sharply. Further increases in P_{CO} cause little change in both E and ΔT. This region is termed region III. On the other hand, the calculated E using Eq. (2) in the regions shown in Fig. 2 is less than 30 mV, which is much less than the observed one.

Figure 3 shows E and ΔT changes under the conditions where P_{CO} is fixed at 0.3 kPa and 580°K. When P_{O_2} is reduced from an excess amount to a particular value (7.9 kPa in this case), E increases slowly but ΔT remains constant. This portion, and the particular P_{O_2} point at a given P_{CO}, respectively, correspond to region I and B_{12} in Fig. 2. Further decreases in P_{O_2} cause E to oscillate and ΔT to decrease monotonically. With decreasing P_{O_2}, furthermore, E stops abruptly oscillating and ΔT moves sharply toward zero at a point corresponding to B_{23}. It enters into region III, where E is about 0.7 V and ΔT is very small.

The ΔT dependence on P_{CO} and P_{O_2} in Figs. 2 and 3 is such that the reaction rate in region I, v_e(I), can be expressed as

$$v_e(\mathrm{I}) = k_e(\mathrm{I})P_{CO}. \qquad (4)$$

Here, k_e(I) is a rate constant. But the rate law in region III, v_e(III), cannot be obtained from the results in Figs. 2 and 3. However, the results obtained with the aid of a closed circulating system in which the reaction rate was measured by a pressure change (*4*), gave v_e(III) as

$$v_e(\mathrm{III}) = k_e(\mathrm{III})P_{O_2}/P_{CO}. \qquad (5)$$

Here, again, k_e(III) is a rate constant.

These rate equations for the deposited Pt in both regions I and III are very similar to those obtained for polycrystalline or single crystalline Pt under UHV conditions (*11, 16, 17*). The activation energies for k_e(I) and k_e(III) were about zero and 125 kJ/mol, respectively. These values are also close to those obtained under UHV conditions (*16, 18*).

b. Gas Composition at B_{12}, B_{23}, and M_e for Deposited Pt

The gas composition at B_{12} could be determined only with low precision, for it was somewhat difficult to determine whether E oscillated or not. This was because the oscillation amplitudes near B_{12} were very small, often less than 1 mV, and almost no regularity was shown.

On the other hand, the partial pressures, P_{CO} and P_{O_2}, at B_{23} were easy to determine. They were more reproducible than those at B_{12} if the partial pressures were changed in

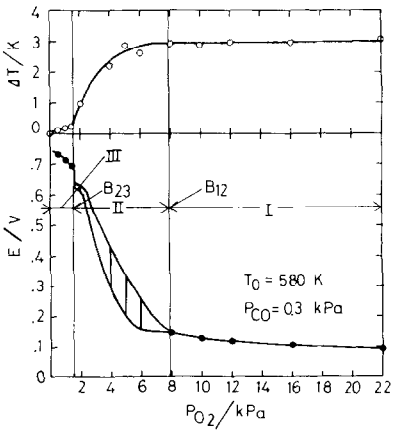

FIG. 3. E and ΔT for solid electrolyte concentration cell with fixed P_{CO}.

the same direction. The P_{CO} at B_{23} that was obtained when P_{CO} was increased with a fixed P_{O_2} was generally higher than that obtained when P_{CO} was reduced.

Figure 4 shows the gas compositions for both B_{12} and B_{23} at 633°K. The gas composition at M_e, which is the point of maximum ΔT, is also included in the figure. The dashed line is the one extended from the plots for M_e, because it was difficult to determine the M_e at a lower P_{CO} or P_{O_2}. The gas composition at B_{23} in this figure was determined under conditions where P_{CO} was reduced or P_{O_2} increased. This value was more appropriate for isothermal plotting than that determined when P_{CO} was increased or P_{O_2} reduced.

The P_{CO} dependences on P_{O_2} at B_{12}, B_{23}, and M_e are similar. They all can be expressed as one formula:

$$P_{CO}/P_{O_2}{}^{\alpha} = b_{12} \text{ (or } b_{23} \text{ or } m_e), \quad (6)$$

where $\alpha = 0.62 \pm 0.06$, and b_{12}, b_{23}, and m_e are the constants for B_{12}, B_{23}, and M_e at a given temperature.

Figure 5 shows the temperature dependence of P_{CO} at both B_{12} and B_{23} with P_{O_2} = 1 kPa. The P_{CO} at M_e with P_{O_2} = 1 kPa was so difficult to determine that it is not shown in this figure. At higher temperatures, above about 720°K, the P_{CO} magnitudes at both B_{12} and B_{23} approach the same value, 2 kPa, which is a stoichiometric P_{CO} in the oxidation. At lower temperatures, the P_{CO}

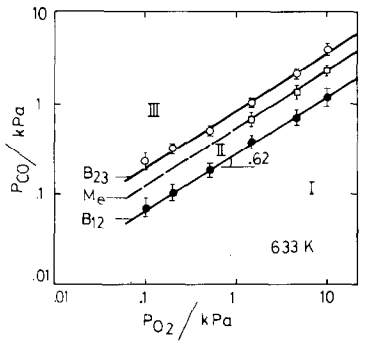

FIG. 4. Gas compositions at B_{12}, B_{23}, and M_e for deposited Pt of solid electrolyte concentration cell. B_{12}, B_{23}: see Fig. 2; M_e: a point of maximum ΔT.

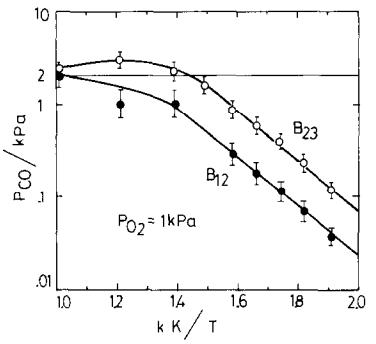

FIG. 5. Arrhenius plots for P_{CO} at B_{12} and B_{23}, with fixed P_{O_2} for deposited Pt.

values at both B_{12} and B_{23} decrease with decreasing temperature. The slope of the Arrhenius plots is 54 kJ/mol. This value is similar to that obtained by Turner *et al.* (*14*). Below 520°K, it became very difficult to measure E, because the impedance of the sample increased to too large an extent.

c. CO Oxidation on Dispersed Pt

Figure 6 shows a typical infrared absorption spectrum obtained during a steady-state kinetic run at 395°K, where P_{O_2} = 10 kPa and P_{CO} = 1 kPa on a pellet of dispersed Pt/stabilized-ZrO_2. Two bands attributable to the chemisorbed species are

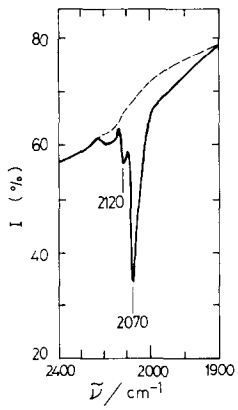

FIG. 6. Typical spectrum for CO adsorbed on dispersed Pt (3 wt%) on Y_2O_3-stabilized ZrO_2 during oxidation in the range 1900–2400 cm^{-1}. Bands at 2120 cm^{-1} (Pt^{2+}–CO); 2070 cm^{-1} (Pt–CO); P_{O_2} = 10 kPa, P_{CO} = 1 kPa, T_O = 395°K. I: transmittance, $\tilde{\nu}$: wavenumber.

observable in the wavenumber range between 1900 and 2400 cm^{-1}. Based on the observations by Eischens and Pliskin (*19*) and by Heyne and Tompkins (*20*), the band at 2070 cm^{-1} is assigned to CO adsorbed on the reduced Pt sites, and the band at 2120 cm^{-1} to CO adsorbed on the oxidized Pt^{2+} sites.

The 2070-cm^{-1} band could be removed when P_{CO} was decreased below a certain value (0.25 kPa in this case), while the 2120-cm^{-1} band did not alter even after the CO supply was stopped. Similar results were obtained by Heyne and Tompkins (*20*) and by Chang and Hegedus (*21*). The peak wavenumber of these two bands remained almost constant within an experimental error of 2 cm^{-1} during the oxidation and after the oxygen supply was stopped. This behavior is consistent with the results obtained by Cant and Donaldson (*22*) and by Cochran *et al.* (*23*). On the basis of these observations, the relative concentration of reactive CO adsorbed on Pt, N_{CO}, was determined by the absorbance ratio, ln (I_0/I) to ln (I_0/I) (s) at 2070 cm^{-1} (I and I_0 being the apparent transmittance with and without gaseous CO and ln (I_0/I) (s) signifying ln (I_0/I) at the saturated adsorption of CO). This was in view of the fairly good linear relation between the absorbance and N_{CO} (*15, 20*).

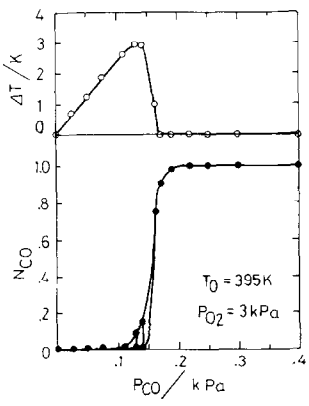

FIG. 7. ΔT and N_{CO} for dispersed Pt with fixed P_{O_2}. N_{CO}: relative surface CO concentration determined by the absorbance ratio, ln (I_0/I) to ln (I_0/I) (s) at 2070 cm^{-1}; I: apparent transmittance with gaseous CO; I_0: apparent transmittance without gaseous CO; ln (I_0/I) (s): ln (I_0/I) at the saturated adsorption of CO.

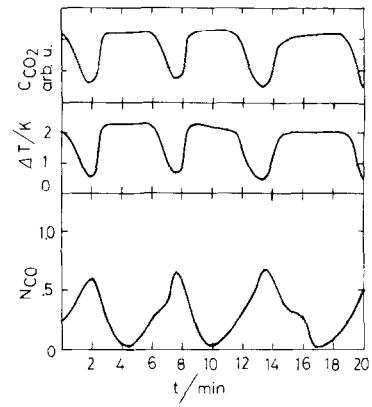

FIG. 8. Typical oscillations in ΔT, N_{CO}, and C_{CO_2} for dispersed Pt. P_{O_2} = 20 kPa, P_{CO} = 0.1 kPa, T_0 = 365°K, C_{CO_2}: CO_2 content in the effluent.

Typical simultaneous infrared and kinetics results are shown in Fig. 7 for the CO oxidation at 395°K, P_{O_2} = 3 kPa. As P_{CO} is increased from zero, ΔT increases linearly with P_{CO} until it shows a maximum, while N_{CO} is almost zero. At the point of maximum ΔT, labeled M_d, N_{CO} increases sharply to high values. Further increases in P_{CO} result in a sharp decrease in ΔT, and a sharp increase in N_{CO} until another P_{CO} point (0.16 kPa in this case). When P_{CO} is higher than that for this point, the rate becomes too small to determine by means of the ΔT measurement. N_{CO} remains almost constant, and did not change even after the oxygen supply was stopped.

Around the point of M_d, ΔT and N_{CO} show oscillations when P_{O_2} is sufficiently high, such as above 3 kPa. Sustained oscillations on dispersed Pt were also observed by McCarthy *et al.* (*12*). Figure 8 illustrates typical oscillation modes for ΔT, N_{CO}, and CO_2 content in the effluent (C_{CO_2}). The value C_{CO_2} is a calculated one on the basis of other experimental results of ΔT and C_{CO_2} using a differential reactor. The ΔT period is about 6 min, which is the same as for N_{CO}. The oscillation modes, however, are somewhat different. We shall be investigating this problem.

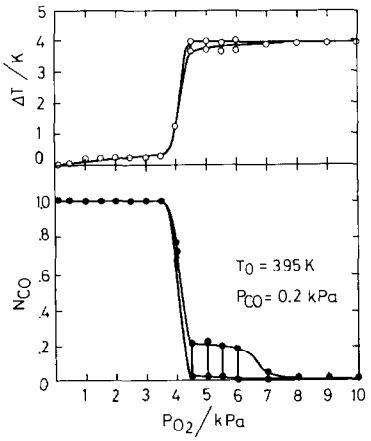

FIG. 9. ΔT and N_{CO} for dispersed Pt with fixed P_{CO}.

Figure 9 shows simultaneous infrared and kinetics results for oxidation with a fixed P_{CO}. When P_{O_2} starts out low and then is increased to a certain value (3.5 kPa in this case), ΔT increases linearly with P_{O_2}. Meanwhile N_{CO} remains constant. Above $P_{O_2} = 3.5$ kPa, a sharp increase in ΔT and a sharp decrease in N_{CO} are observed, accompanied by their oscillations. Further increases in P_{O_2} cause ΔT to become independent of P_{O_2}. No N_{CO} is detected.

Based on the results obtained from Figs. 7 and 9, the reaction rate in the oxygen-rich or CO-poor region, which corresponds to region I for the deposited Pt, labeled $v_d(I)$, is given by

$$v_d(I) = k_d(I)P_{CO}. \quad (7)$$

Here $k_d(I)$ is a rate constant. The rate equation in the oxygen-poor or CO-rich region, which corresponds to region III for the deposited Pt, labeled $v_d(III)$, can be given on the basis of the results obtained from Fig. 9 and with the aid of a closed circulating system (4). It can be written as:

$$v_d(III) = k_d(III)P_{O_2}/P_{CO}, \quad (8)$$

where $k_d(III)$ is a rate constant. The activation energies for $k_d(I)$ and $k_d(III)$ were zero and 108 kJ/mol, respectively. Thus, the rate equations and activation energies for the dispersed Pt were almost the same as those for the deposited Pt. This fact has already been pointed out by Engel and Ertl (*10*).

d. Gas Composition at M_d

The E oscillation on deposited Pt was easy to recognize, while those in both ΔT and absorbance at 2070 cm^{-1} on dispersed Pt were hard to define. This is because experimental errors there were greater, the oscillation periods generally larger, and regularities poorer than for E. Moreover, the oscillations in ΔT and absorbance at 2070 cm^{-1} were not found for lower P_{O_2} values nor for higher temperatures, such as 470°K. That is to say, it is very difficult to determine either B_{12} or B_{23} for the dispersed Pt on the basis of ΔT or absorbance at 2070 cm^{-1}.

Figure 4 showed that, for the deposited Pt, M_e behaved like B_{12} and B_{23}, where the transition occurred between oscillatory and nonoscillatory regions. Thus for the dispersed Pt a point similar to M_e for the deposited Pt, labeled M_d, was used in order to obtain an indication about the boundaries of region II. M_d was comparatively easy to determine, for at this point the reaction rate was maximized, and N_{CO} was more than zero even at its lowest value if it oscillated. The absorbance at 2070 cm^{-1}, or N_{CO}, was more useful (especially for lower oxygen partial pressures) than rate or ΔT. At higher temperatures, such as 470°K, the P_{CO} at M_d under conditions where P_{CO} was increased with a fixed P_{O_2}, was higher than that under conditions where P_{CO} was reduced. This was mainly because the Pt surface temperature in the former case was higher than that in the latter case. Here, the M_d in the former case was adopted.

Figure 10 shows the gas composition at the transition point, M_d, at 365°K. Reproducibility was about 10% on repeated runs. P_{CO} dependence on P_{O_2} at M_d is expressed as:

$$P_{CO}/P_{O_2}{}^{\beta} = m_d \quad (9)$$

where $\beta = 0.60 \pm 0.06$, and m_d is a constant for M_d at a given temperature. This relation

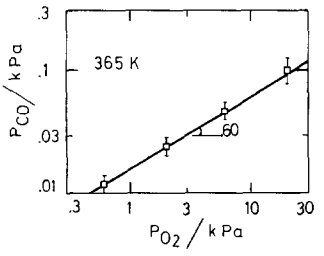

FIG. 10. Gas compositions at M_d for dispersed Pt. M_d: transition point where ΔT is maximized and N_{CO} is more than zero even at its lowest value if it oscillates.

is quite similar to that for, B_{12}, B_{23}, or M_e for the deposited Pt, though the P_{CO} at M_d is much higher.

The temperature dependence of the P_{CO} at the transition point with P_{O_2} = 1 kPa is shown in Fig. 11. At higher temperatures, such as 500°K, the P_{CO} at M_d approaches 2 kPa, which is the stoichiometric pressure of CO in the oxidation. At lower temperatures at least down to 300°K, the P_{CO} at M_d decreases with decreasing temperature, and the slope of the Arrhenius plots is 54 kJ/mol. This is a very similar value to that for B_{12} or B_{23} with the deposited Pt.

DISCUSSION

First, the mechanism for emf generation will be considered. Some comments on the reaction mechanism for CO oxidation on Pt will then be made on the basis of the results of the emf measurements.

a. Mechanism for emf Generation

In region I where the rate equation was expressed as $k(\mathrm{I})P_{CO}$, E was comparatively small and no surface CO (N_{CO}) was detected by means of infrared spectroscopy. In region III where the rate equation was given by $k(\mathrm{III})P_{CO_2}/P_{CO}$, E was very large and showed little change. Here, N_{CO} was equal to that at the saturated adsorption in the absence of oxygen. In region II where the rate showed a maximum against a P_{CO} change, E oscillated. The value N_{CO} also oscillated, at least in the presence of a sufficient amount of oygen. On the basis of these results, it is reasonable to think that E correlates with N_{CO} during CO oxidation over the whole range of the gas composition.

This correlation can be confirmed by several facts. The relation between P_{CO} and P_{O_2} at B_{12} or B_{23} was almost the same as that at M_d. As was mentioned in the previous section, B_{12} and B_{23} are transition points between the oscillatory and nonoscillatory regions, and were determined by E. M_d indicates the same transition, and was determined mainly by N_{CO} through the use of infrared spectroscopy. The temperature dependences of the relations were also the same. Thus it was concluded that E correlates with N_{CO} during CO oxidation on Pt.

Since the application of a solid electrolyte concentration cell to the study of heterogeneous catalysis was proposed by Wagner (*5*), the E of a zirconia galvanic cell type (1) has been considered to show only the activity of oxygen on a Pt electrode during the reaction (*6–8*). Figure 2 shows, however, that the E in region I, e.g., for P_{CO} = 0.1 kPa and P_{O_2} = 5 kPa at 603°K, was about 100 mV larger than that in the absence of CO. If this E difference was due only to the activity of oxygen on Pt, then according to the concentration cell equation, this oxygen activity must be reduced less than one-thousandth when a very small amount of CO was added to the gas containing sufficient O_2. This is quite unreasonable, mainly because the CO oxidation

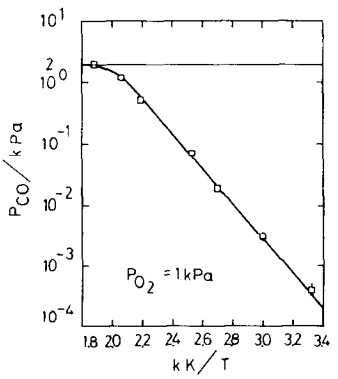

FIG. 11. Arrhenius plots showing P_{CO} at M_d with fixed P_{O_2} for dispersed Pt.

rate is independent of P_{O_2}. Moreover it is impossible that the Pt surface becomes almost clean when such a scarce amount of CO compared to oxygen is introduced. Golchet and White (*11*) and Matsushima (*17*) have reported that even at very low pressures of the order of 10^{-5} Pa, the oxygen coverages on Pt were reduced to only about one-half when the amount of CO corresponding to that in region I was added.

Needless to say, the reaction on Pt is not in equilibrium. If it were, the E increase would have to be on the order of 0.1 mV.

This consideration led to the belief that E is caused by a mixed-electrode potential at the mixed-gas electrode (*3, 4*). The mixed electrode potential is brought about by reactions near a triple contact Pt-stabilized ZrO_2-gas, e.g.,

$$O\sigma + 2e^- \rightleftarrows O^{2-} + \sigma \qquad (10)$$

$$CO\sigma + O^{2-} \rightleftarrows CO_2 + 2e^- + \sigma. \qquad (11)$$

Here $O\sigma$ and $CO\sigma$ represent oxygen and CO adsorbed on Pt during the reaction, respectively; e^- is an electron in Pt, O^{2-} is an oxide ion in stabilized ZrO_2 and σ is a vacant site on Pt. More specifically, E is determined not only by oxygen, but also by CO adsorbed on a Pt electrode.

If these electrochemical reactions do not disturb the CO oxidation catalyzed by Pt, which was indirectly checked in the previous section, then $O\sigma$ and $CO\sigma$ represent the surface concentration during the oxidation regardless of the progress of the electrochemical reactions. Thus, E indicates the surface adsorption states of CO and oxygen on Pt during the reaction. In this respect, a solid electrolyte concentration cell is useful for studying rapid changes in the surface adsorption states of a heterogeneous catalyst during a reaction especially under atmospheric pressure. A detailed report on the quantitative treatment will be presented subsequently.

b. Reaction Mechanism of CO Oxidation

E measurement by use of a solid electrolyte concentration cell is especially useful in the study of very small amounts of adsorption during the reaction, because the mixed electrode potential is sensitive to reactants. For example, even in region I, a low P_{CO} in a high P_{O_2} should yield surface CO as described previously, though its amount was so small that it was not detected by means of infrared spectroscopy. Therefore, the CO oxidation must proceed via a Langmuir–Hinshelwood mechanism including the surface reaction process between the adsorbed species. This process is not a rate-determining step, because N_{CO} is very small, and the reaction rate is independent of P_{O_2}. This conclusion is consistent with both conclusions obtained at very low pressures (*17, 24–26*) and at high pressures (*22, 27*).

The P_{CO} at B_{23} with a fixed P_{O_2}, which was related to the occurrence of the oscillations, had an activation energy of 54 kJ/mol. This value is about half the activation energy for the oxidation in region III, 125–108 kJ/mol. The latter value is almost the same as the desoprtion energy of CO, 126 kJ/mol (*16, 18, 28, 29*). This relation has been pointed out earlier by Bonzel and Ku (*16*). It is often assumed that the activation energy for surface diffusion is roughly half the desorption energy (*24, 30*). Thus, B_{23} can be considered to be related to the surface diffusion of CO. That is to say, the occurrence of oscillations is thought to be caused by the surface state in which CO adsorbed becomes mobile.

The dependence of P_{CO} on P_{O_2} at B_{12}, B_{23}, M_e, or M_d was almost the same (Eqs. (6) and (9)), or $P_{CO}/P_{O_2}^{0.62}$ = const. Studies at very low pressure (*11, 16, 17*) and those concerning oscillations (*13, 14*) have often been related to the simple partial pressure ratio, P_{CO}/P_{O_2}. The relation observed here has never appeared in any literature. However, Golchet and White (*11*) pointed out that the partial pressure ratio, P_{CO}/P_{O_2}, at the point of transition between the first-order P_{CO} and inhibition regions at very low pressures, shifted from about 1 to about 0.1

at high pressures. This relation may therefore be considered to connect the field of surface science with that of real catalysts. A detailed study of this behavior is in progress.

ACKNOWLEDGMENTS

The authors express their appreciation to Professor K. Tamaru and Dr. M. Kawai for their valuable comments.

REFERENCES

1. Fleming, W. J., *J. Electrochem. Soc.* **124,** 21 (1977).
2. Hetrick, R. E., and Logothetis, E. M., *Appl. Phys. Lett.* **34,** 117 (1979).
3. Okamoto, H., Obayashi, H., and Kudo, T., *Solid State Ionics* **1,** 319 (1980).
4. Okamoto, H., Obayashi, H., and Kudo, T., *Solid State Ionics* **3/4,** 453 (1981).
5. Wagner, C., *Adv. Catal.* **21,** 323 (1970).
6. Vayenas, C., and Saltsburg, H., *J. Catal.* **57,** 296 (1979).
7. Vayenas, C. G., Lee, B., and Michaels, J., *J. Catal.* **66,** 36 (1980).
8. Haaland, D. M., *J. Electrochem. Soc.* **127,** 796 (1980).
9. Tamura, K., *Adv. Catal.* **15,** 65 (1964).
10. Engel, T., and Ertl, G., *Adv. Catal.* **28,** 1 (1979).
11. Golchet, A., and White, J. M., *J. Catal.* **53,** 266 (1978).
12. McCarthy, E., Zahdradnik, J., Kuczynski, G. C., and Carberry, J. J., *J. Catal.* **39,** 29 (1975).
13. Dauchot, J. P., and Van Cakenberghe, J., *Jpn. J. Appl. Phys. Suppl. Part 2* **2,** 533 (1974).
14. Turner, J. E., Sales, B. C., and Maple, M. B., *Surf. Sci.* **103,** 54 (1981).
15. Heyne, H., and Tompkins, F. C., *Proc. Roy. Soc. London* **292,** 460 (1966).
16. Bonzel, H. P., and Ku, R., *J. Vac. Sci. Technol.* **9,** 663 (1972).
17. Matsushima, T., *Bull. Chem. Soc. Jpn.* **51,** 1956 (1978).
18. Pacia, N., Cassuto, A., Pentenero, A., and Weber, B., *J. Catal.* **41,** 455 (1976).
19. Eischens, R. P., and Pliskin, W. A., *Adv. Catal.* **10,** 2 (1958).
20. Heyne, H., and Tompkins, F. C., *Trans. Faraday Soc.* **63,** 1274 (1967).
21. Chang, C. C., and Hegedus, L. L., *J. Catal.* **57,** 361 (1979).
22. Cant, N. W., and Donaldson, R. A., *J. Catal.* **71,** 320 (1981).
23. Cochran, H. D., Donnelly, R. G., Modell, M., and Baddour, R. F., *Colloid Interface Sci.* **3,** 131 (1976).
24. Palmer, R. L., and Smith, J. N., Jr., *J. Chem. Phys.* **60,** 1453 (1974).
25. Matsushima, T., *J. Catal.* **55,** 337 (1978).
26. Strozier, J. A., Jr., *Surf. Sci.* **87,** 161 (1979).
27. Herz, R. K., and Marin, S. P., *J. Catal.* **65,** 281 (1980).
28. Weinberg, W. H., Comrie, C. M., and Lambert, R. M., *J. Catal.* **41,** 489 (1976).
29. Morgan, A. E., and Somorjai, G. A., *J. Chem. Phys.* **51,** 3309 (1969).
30. Hopster, H., Ibach, H., and Comsa, G., *J. Catal.* **46,** 37 (1977).